Chemical Science

EDGE ARTICLE

View Article Online
View Journal | View Issue

Cite this: *Chem. Sci.*, 2019, **10**, 10366

All publication charges for this article have been paid for by the Royal Society of Chemistry

Received 25th July 2019
Accepted 17th September 2019

DOI: 10.1039/c9sc03758f

rsc.li/chemical-science

Aerobic C–C and C–O bond formation reactions mediated by high-valent nickel species†

Sofia M. Smith,[b] Oriol Planas,[c] Laura Gómez,[d] Nigam P. Rath,[e] Xavi Ribas[c] and Liviu M. Mirica*[ab]

Nickel complexes have been widely employed as catalysts in C–C and C–heteroatom bond formation reactions. While Ni(0), Ni(I), and Ni(II) intermediates are most relevant in these transformations, recently Ni(III) and Ni(IV) species have also been proposed to play a role in catalysis. Reported herein is the synthesis, detailed characterization, and reactivity of a series of Ni(II) and Ni(III) metallacycle complexes stabilized by tetradentate pyridinophane ligands with various N-substituents. Interestingly, while the oxidation of the Ni(II) complexes with various other oxidants led to exclusive C–C bond formation in very good yields, the use of O_2 or H_2O_2 as oxidants led to formation of appreciable amounts of C–O bond formation products, especially for the Ni(II) complex supported by an asymmetric pyridinophane ligand containing one tosyl N-substituent. Moreover, cryo-ESI-MS studies support the formation of several high-valent Ni species as key intermediates in this uncommon Ni-mediated oxygenase-type chemistry.

Introduction

The formation of C–C and C–heteroatom bonds plays a fundamental role in organic transformations, and C–C cross-coupling reactions are among the most powerful tools for the construction of new C–C bonds.[1–3] In this context, nickel catalysts have been commonly used for more than four decades in cross-coupling reactions such as Negishi, Kumada and Suzuki couplings.[4–9] The most common oxidation states involved in these catalytic transformations are Ni^0, Ni^I, and Ni^{II}, although more recent studies show that Ni^{III} and Ni^{IV} oxidation states can also play a role in C–C bond formation.[10–20] By comparison, stoichiometric and catalytic Ni-mediated C–heteroatom bond formation reactions have been developed mostly in the past two decades.[21–36]

In the past several years we have employed tetradentate pyridinophane ligands to stabilize uncommon organometallic $Pd^{III/IV}$ and $Ni^{III/IV}$ complexes,[37–44] which can undergo C–C and C–heteroatom bond formation reactions. In addition, we have recently reported the use of the ligand 1,4,7-trimethyl-1,4,7-triazacyclonane (Me_3tacn) to stabilize high-valent $Ni^{III/IV}$ complexes that undergo C–C and C–heteroatom bond formation reactions.[35] With this ligand, small amounts of C–O bond formation products (~5%) were observed upon oxidation of $(Me_3tacn)Ni^{II}(CH_2CMe_2\text{-}o\text{-}C_6H_4)$ with O_2.[35] Herein, we report the use of modified pyridinophane ligands that directly affects that stability and reactivity of the corresponding high-valent Ni complexes. We tested the effect of the amine N-substituents by replacing the methyl groups with a more electron-withdrawing toluenesulfonyl (tosyl, Ts) group or a bulkier *tert*-butyl (*t*Bu) group. By employing a Ni-cycloneophyl structure motif, we have been able to isolate Ni^{III} species and also perform uncommon oxidatively-induced C–C and C–O bond formation reactions using O_2 or H_2O_2 as the oxidants. The ability to control the relative reactivity of C–C *vs.* C–heteroatom bond formation should have important implications in various organic transformations.

Results and discussion

Synthesis and characterization of $Ni^{II/III}$ complexes

The ligands *N*,*N*′-dimethyl-2,11-diaza[3.3](2,6)pyridinophane (^{Me}N4), *N*,*N*′-tosylmethyl-2,11-diaza[3.3](2,6)pyridinophane (^{TsMe}N4), *N*,*N*′-ditosyl-2,11-diaza[3.3](2,6)pyridinophane (^{Ts}N4) and *N*,*N*′-di-*tert*-butyl-2,11-diaza[3.3](2,6)pyridinophane (^{tBu}N4) were synthesized according to literature procedures.[45,46] With these ligands a series of cycloneophyl complexes were synthesized through a ligand exchange of $(py)_2Ni^{II}$(cycloneophyl).[47,48] The orange Ni^{II} complex (^{Me}N4)Ni^{II}(cycloneophyl), **1**, was

[a]*Department of Chemistry, University of Illinois at Urbana-Champaign, 600 S. Mathews Avenue, Urbana, Illinois 61801, USA. E-mail: mirica@illinois.edu*
[b]*Department of Chemistry, Washington University in St. Louis, One Brookings Drive, St. Louis, Missouri 63130-4899, USA*
[c]*Departament de Química, Institut de Química Computacional i Catàlisi (IQCC), Universitat de Girona, Campus de Montilivi, Girona E-17003, Catalonia, Spain*
[d]*Serveis Tècnics de Recerca (STR), Universitat de Girona, Parc Científic i Tecnològic, Girona E-17071, Catalonia, Spain*
[e]*Department of Chemistry and Biochemistry, University of Missouri-St. Louis, One University Boulevard, St. Louis, Missouri 63121-4400, USA*

† Electronic supplementary information (ESI) available: Synthetic details, spectroscopic characterization, stoichiometric and catalytic reactivity studies, and crystallographic data. CCDC 1943288–1943290. For ESI and crystallographic data in CIF or other electronic format see DOI: 10.1039/c9sc03758f

prepared in a 72% yield (Scheme 1),[49] while the yellow Ni^{II} complex (^{TsMe}N4)Ni^{II}(cycloneophyl), **2**, was prepared in 81% yield and fully characterized.[50] The cyclic voltammetry (CV) characterization of **2** reveals two main oxidation events at −990 mV and 750 mV *vs.* Fc^+/Fc, along with a smaller oxidation wave at 70 mV (Table 1).[50] The two main oxidation events are tentatively assigned to the $Ni^{III/II}$ and $Ni^{IV/III}$ redox couples, while the oxidation wave at 70 mV is proposed to correspond to a conformer of complex **2** in which the ^{TsMe}N4 ligand adopts a κ^3 binding mode, while the oxidation wave at −990 mV likely corresponds to the conformation of **2** with ^{TsMe}N4 in a κ^4 binding mode.[29,35] The third complex, (^{Ts}N4)Ni^{II}(cycloneophyl), **3**, was prepared in a 67% yield and was fully characterized by ^{1}H NMR and ^{13}C NMR.[50] Its CV shows an oxidation potential at −400 mV, which is tentatively assigned to the $Ni^{III/II}$ couple. Finally, the yellow Ni^{II} complex (^{tBu}N4)Ni^{II}(cycloneophyl), **4**, was prepared in 73% yield and was also characterized by ^{1}H NMR and ^{13}C NMR.[50] The CV of **4** shows a first oxidation potential at 200 mV *vs.* Fc^+/Fc, which is higher than those observed for **2** and **3**, likely due to the steric bulk of the *t*-butyl group, and as observed previously.[37,39–41,44]

Given their accessible oxidation potentials, complexes **1–4** can easily be oxidized with one equivalent of acetylferrocenium tetrafluoroborate (^{Ac}FcBF$_4$) or silver hexafluoroantimonate ($AgSbF_6$) in THF at −50 °C to yield [(^{TsMe}N4)Ni^{III}(cycloneophyl)]$^+$, **2**$^+$, [(^{Ts}N4)Ni^{III}(cycloneophyl)]$^+$, **3**$^+$, and [(^{tBu}N4)Ni^{III}(cycloneophyl)]$^+$, **4**$^+$. The X-ray structures of both **2**$^+$ and **3**$^+$ reveal six-coordinate Ni^{III} centers in distorted octahedral geometries (Fig. 1). For **2**$^+$, the Ni–N_{Ts} bond length 2.527 Å is larger than the Ni–N_{Me} bond length 2.199(4) Å, given that the *N*-tosyl group is more electron withdrawing *vs.* the *N*-methyl group. The Ni–N_1 bond length of 2.182(5) Å is larger than the Ni–N_2 bond of 1.867(4) Å due to a stronger trans effect of the C(sp^3) *vs.* the C(sp^2) donor atom. Similar trends are observed for **3**$^+$, while the Ni–N_{Ts} distances are significantly longer than the axial interactions observed for **2**$^+$ (Fig. 1).

The EPR spectrum of **2**$^+$ exhibits a rhombic signal with a superhyperfine coupling observed in the g_z direction due to one axial N donors ($I = 1$) coupling to the Ni^{III} center (Fig. 2), suggesting that the N_{Ts} atom only weakly coordinates in the axial position. By comparison, complex **3**$^+$ exhibits a rhombic signal with a weak superhyperfine coupling to two N atoms in the g_z direction ($A_{2N} = 8$ G), suggesting that both N_{Ts} atoms weakly bind to the Ni center (Fig. 2). Also, a small amount of unknown Ni^{III} impurity is present in complex **3**$^+$, and simulation of the experimental spectrum suggests this impurity amounts to ∼5% of the entire EPR signal. Complex **4**$^+$ also exhibits a rhombic EPR signal, with superhyperfine coupling to two axial N donors in the g_z direction ($A_{2N} = 11$ G), suggesting that the *N*-*t*-butyl groups interact with the Ni center to a greater extent than the *N*-Ts groups in **3**$^+$.

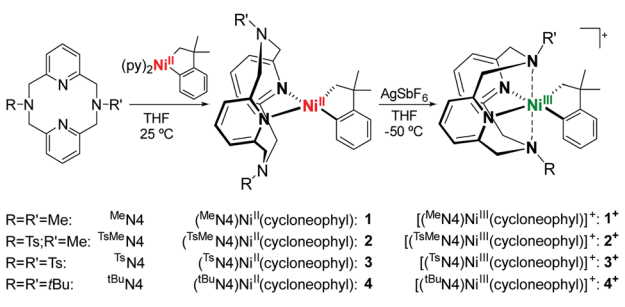

Scheme 1 Synthesis of ($^{RR'}$N4)Ni(cycloneophyl) complexes.

Table 1 Cyclic voltammetry (CV) data for (^{R}N4)Ni(cycloneophyl) complexes

Complex	**1**	**2**	**3**	**4**
$E(Ni^{II/III})^a$ (mV)	−1700	−990	−400	200

[a] $E(Ni^{II/III})$ values reported *vs.* Fc^+/Fc 0.1 M nBu_4NPF_6/MeCN at RT, 100 mV s^{-1} scan rate.

C–C and C–X bond formation reactivity of (^{R}N4)Ni^{II}(cycloneophyl) complexes

With the new (^{R}N4)Ni^{II}(cycloneophyl) complexes in hand, we set out to probe their reactivity in C–C and C–heteroatom bond formation reactions. First, we studied the oxidation of complexes **1–4** with 1-fluoro-2,4,6-trimethylpyridinium triflate (NFTPT), 5-(trifluoromethyl)dibenzothiophenium trifluoromethanesulfonate (TDTT), xenon difluoride (XeF_2) and (diacetoxyiodo)benzene ($PhI(OAc)_2$), since these oxidants have been commonly employed in high-valent transition metal chemistry, including Ni complexes.[18,19,51–54] While no C–heteroatom bond formation was detected, the C–C coupled product 1,1-dimethylbenzocyclobutene was obtained in various yields (Table 2).[50] Comparing the reactivity of complexes **1–4**, it appears that the presence of electron withdrawing *N*-Ts groups leads to higher C–C product yields, with up to 99% conversion

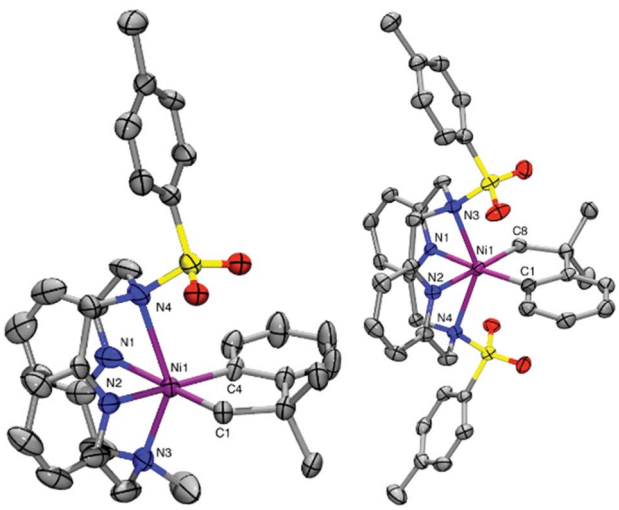

Fig. 1 ORTEP representation of **2**$^+$ (left) and **3**$^+$ (right) with 50% probability thermal ellipsoids. Selected bond distances (Å), **2**$^+$: Ni1–C1, 1.938(9); Ni1–C4, 1.938(4); Ni1–N1, 2.182(5); Ni1–N2, 1.867(4); Ni1–N3, 2.199(4); Ni1–N4, 2.527; **3**$^+$: Ni1–C1, 1.933(3); Ni1–C8, 1.982(3); Ni1–N1, 1.993(3); Ni1–N2, 2.010(3); Ni1–N3, 2.360(3); Ni1–N4, 2.436(3).

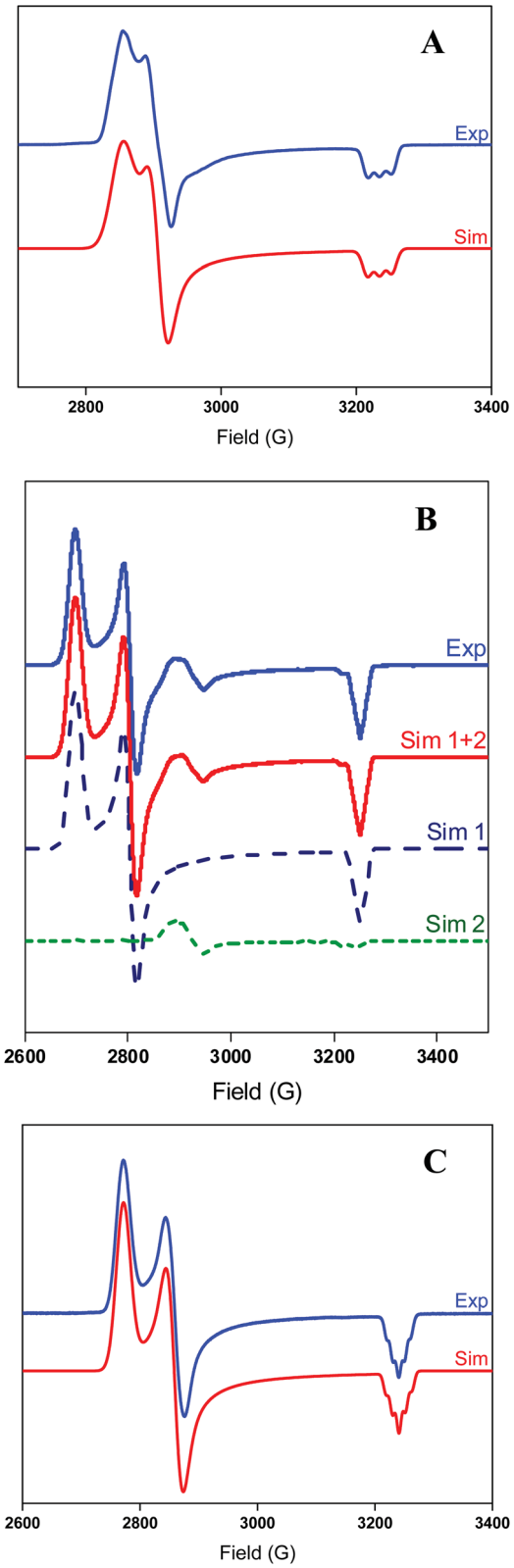

Fig. 2 Experimental (1 : 3 MeCN : PrCN, 77 K) and simulated EPR spectra of 2^+ ((A) top) using the following parameters: $g_x = 2.277$, $g_y = 2.235$, $g_z = 2.009$ (A_z(N) = 18.0 G). Experimental (1 : 3 MeCN : PrCN, 77 K) and simulated EPR spectra of 3^+ ((B) middle) using the following parameters for sim 1: $g_x = 2.409$, $g_y = 2.318$, $g_z = 2.000$ (A_z(2N) = 8.0 G) and sim 2: $g_x = 2.253$, $g_y = 2.220$, $g_z = 2.010$ (A_z(N) = 18.0 G). Simulations 1 and 2 were added in a 19 : 1 ratio respectively to simulate the experimental spectra properly. Experimental (1 : 3 MeCN : PrCN, 77 K) and simulated EPR spectra of 4^+ ((C) bottom) using the following parameters: $g_x = 2.345$, $g_y = 2.273$, $g_z = 2.006$ (A_z(2N) = 11.0 G).

observed when **3** was oxidized with XeF_2. This reactivity trend is likely due to the coordination of the amine arms to create a six-coordinate high-valent Ni species that is less reactive towards reductive elimination than a five- or four-coordinate Ni species formed in the presence of the ligands with weakly interacting *N*-Ts groups. Since the reagents employed above are considered to usually act as two-electron oxidants, we tentatively propose the formation of transient (^{R}N4)Ni^{IV}(cycloneophyl) species that then undergo C–C reductive elimination to generate the 1,1-dimethylbenzocyclobutene product and a (^{R}N4)Ni^{II}-bis-solvento species, similar to what we observed recently for the (Me_3tacn)Ni^{IV}(cycloneophyl) system.[35]

We have also investigated the oxidation of complexes **1–4** with O_2 and H_2O_2. The use of O_2 and H_2O_2 as an oxidant obviates the requirement for strong and hazardous oxidants which generate undesired stoichiometric byproducts, and thus making O_2 and H_2O_2 "greener" reagents for C–C and C–O bond formation reactions. The exposure of solutions of complexes **1–4** to O_2 quickly generates orange or red solutions. To our delight, heating these reaction mixtures for 14 hours at 70 °C followed by acidic workup and GC-MS analysis reveals the formation of C–O bond formation products. For example, oxidation of **1** and **3** with O_2 generates C–O bond formation products in 12–17% combined yield, while complex **2** shows up to 41% combined yield of C–O products (Table 3). By comparison, no C–O bond formation was formed for **4**, suggesting that the steric bulk of the *tert*-butyl groups precludes exogenous reactivity, and thus **4** was not employed in any further reactivity studies. The GC-MS analysis also confirmed the presence of C–C coupled product 1,1-dimethylbenzocyclobutene for all four complexes, with up to 69% yield observed for **3**. In addition, the oxidants H_2O_2 and *m*-chloroperoxybenzoic acid (*m*CPBA) are also capable of promoting C–C and C–O bond formation, although lower C–O product yields were observed,[50] likely due to the formation of more stable high-valent Ni species that undergo reductive elimination more slowly or undergo unspecific decomposition (see below). The lower C–O and C–C bond formation product yields might be attributed to the presence of water in the H_2O_2 solution that likely leads to unspecific decomposition of the high-valent Ni species before being able to undergo reductive elimination.[50] Overall, complex **2** seems to be the optimal system to generate the highest yields of C–O products, likely by providing the sweet spot of stability *vs.* reactivity to allow for the oxidation by O_2, and the formation of high-valent Ni species that persists long enough to undergo C–O reductive elimination.

To further probe the mechanism of oxidation, the reaction of (^{R}N4)Ni^{II}(cycloneophyl) complexes **1–3** with O_2 or H_2O_2 was monitored at −50 °C in 9 : 1 acetone-d_6 : D_2O. While no Ni^{IV} intermediates were observed by ^{1}H NMR, the formation of more than one Ni^{III} species was suggested by EPR spectroscopy. In addition, cryo-electrospray mass spectrometry (cryo-ESI-MS)

Table 2 Oxidation of (^{R}N4)Ni^{II}(cycloneophyl) with various oxidants in MeCN

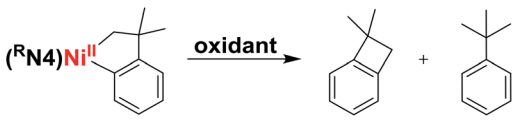

	Yield[a] (%)			
Complex	$PhI(OAc)_2$	NFTPT	TDTT	XeF_2
1	4; 22	17; 39	7; 19	20; 40
2	24; 13	32; 27	33; 15	50; 16
3	42; 10	**96**; 4	42; 9	**99**; 1
4	ND[b]	14; 44	6; 9	ND[b]

[a] Reaction conditions: MeCN, 70 °C, 14 h. Yields (%) were determined by GC-FID *vs.* 1,3,5-trimethoxybenzene as internal standard. The first yield shown is for 1,1-dimethylbenzocyclobutene, while the second yield is for is *tert*-butylbenzene. [b] Not determined.

Table 3 Oxidation of (^{R}N4)Ni^{II}(cycloneophyl) with O_2 in 9 : 1 MeCN : H_2O

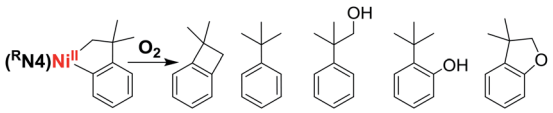

	Yields[a] (%)					Total yield (%)
Complex						
1	35	12	8	3	6	**64**
2	41	12	**2**	**17**	**22**	**94**
3	69	12	2	5	5	**93**
4	27	6	0	0	0	**33**

[a] Reaction conditions: 9 : 1 MeCN : H_2O, 70 °C, 14 h. Yields (%) were determined by GC-FID *vs.* 1,3,5-trimethoxybenzene as internal standard.

was employed in an attempt to detect any high-valent Ni intermediates formed during the oxidation process.[30,55] First, the oxidation of (^{TsMe}N4)Ni^{II}(cycloneophyl) complex **2** with O_2 was probed by cryo-ESI-MS at −80 °C in 9 : 1 acetone : H_2O, followed by addition of $HClO_4$ as the proton source. The most intense signal corresponds to the [(^{TsMe}N4)Ni^{III}(cycloneophyl)]$^+$ species **2**$^+$ (molecular formula $C_{32}H_{36}N_4NiO_2S$, *m*/*z* 598.1912), confirming the detection of Ni^{III} species by EPR. In addition, two less intense species were observed that correspond to the mass of species **2**$^+$ plus two or one O atoms, $C_{32}H_{36}N_4NiO_4S$ (*m*/*z* 630.1811), and $C_{32}H_{36}N_4NiO_3S$ (*m*/*z* 614.1856), respectively. While we cannot unambiguously assign the structure of these species,[50] they are strongly suggesting an inner-sphere aerobic oxidation mechanism that eventually leads to formation of the detected C–O bond formation products.

Interestingly, oxidation of **2** at −80 °C with H_2O_2 in 9 : 1 acetone : H_2O generates a number of transient and persistent species that can be observed by cryo-ESI-MS. The first two transient species that are observed are tentatively assigned to a Ni^{IV}–hydroperoxo and a Ni^{IV}–hydroxo complex (**A**, *m*/*z* 631.1884, and **B**, *m*/*z* 615.1934, Fig. 3).[50] The decay of the two transient species leads to the formation of a persistent species that likely corresponds to a hydroxylated Ni-cycloneophyl species (**C**, *m*/*z* 614.1856). This Ni^{III} species **C** is then proposed to undergo reductive elimination to form a cationic Ni^{I} species **E**, which was detected by ESI-MS, and the cyclized C–O product (Scheme 2). Alternatively, the Ni^{IV} species **B** can

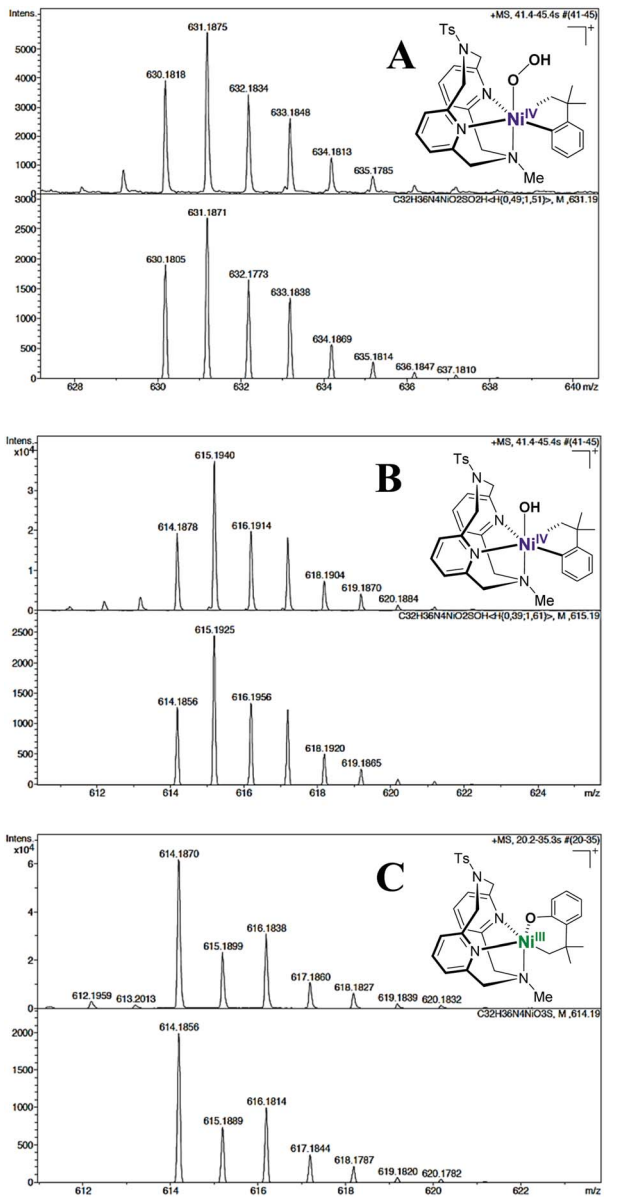

Fig. 3 Cryo-ESI-MS spectra (top) and simulations (bottom) showing the isotopic patterns of cationic Ni^{III} and Ni^{IV} intermediates found during the oxidation of **2** with H_2O_2 in 10% H_2O/acetone and $HClO_4$ at −80 °C. From top to bottom: **A**, [(^{TsMe}N4)Ni^{IV}(cycloneophyl)(OOH)]$^+$ *m*/*z* 631.1884 (transient species, simulated as a 49 : 51 mixture with a **2**$^+$ + O_2 species with *m*/*z* 630.1805), **B**, [(^{TsMe}N4)Ni^{IV}(cycloneophyl)(OH)]$^+$ *m*/*z* 615.1934 (transient species, simulated in a 39 : 61 ratio with species **C**) and **C**, [(^{TsMe}N4)Ni^{III}(−CH_2CMe_2-*o*-C_6H_4−O)]$^+$ *m*/*z* 614.1856 (persistent species).[50]

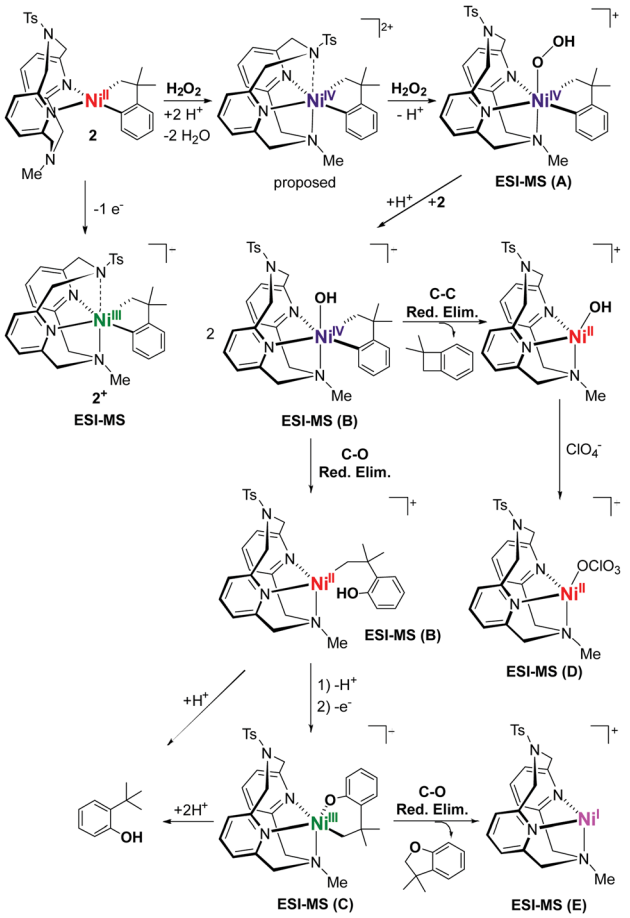

Scheme 2 Proposed mechanism for the oxidatively-induced C–C and C–O bond formation of **2** with H_2O_2 in 10% H_2O/acetone and $HClO_4$ as a proton source.

undergo C–C reductive elimination to generate the 1,1-dimethylbenzocyclobutene product and the $[(^{TsMe}N4)Ni^{II}(MeCN)_2]^{2+}$ complex,[35] which is observed in the ESI-MS as the $[(^{TsMe}N4)Ni^{II}(ClO_4)]^+$ species **D**. Analysis by cryo-ESI-MS of the oxidation of complexes **1** and **3** with H_2O_2 also reveals the formation of the persistent Ni complexes, although no high-valent Ni intermediates were observed in these cases, likely due to their decreased stability.[50] When comparing the product yields for complexes **1**–**3** and the various oxidants employed, the general trend is observed in which the less stable the high-valent Ni species are, the higher are the yields of C–C and/or C–O bond formation products. Overall, these results are very promising, suggesting that with an appropriately tailored multidentate ligand the corresponding organometallic Ni complexes can be oxidized with mild oxidants such as O_2 and H_2O_2 and promote C–C and C–heteroatom bond formation reactivity that is usually possible only under stringent anaerobic and anhydrous conditions. Interestingly, high-valent Ni–oxo species supported by the multidentate amine ligands have also been reported recently,[56] lending support to the transient species proposed above. It is also important to note that similar reactivity with O_2 and H_2O_2 has been observed previously for both Pt and Pd complexes. In those cases, the use of appropriate multidentate N-donor ligands was also essential in promoting the oxidation of organometallic Pt[57–59] and Pd[39,40,42,60,61] complexes with O_2 and H_2O_2 to generate isolable or detectable high-valent 'oxygenated' transition metal species, however their C–heteroatom reductive elimination reactivity is limited.[62] While the mechanistic studies reported herein are preliminary and no high-valent oxygenated Ni species have been isolated, this report strongly suggests that appropriately-designed organometallic Ni complexes can be easily oxidized by oxidants such as O_2 and H_2O_2 in a similar manner to the Pt and Pd species, yet the high-valent Ni species should exhibit increased C–heteroatom reductive elimination reactivity that can be synthetically useful.

Conclusion

In conclusion, we report herein the use of four different pyridinophane ligands to stabilize organometallic Ni complexes, including high-valent Ni species. All isolated complexes were fully characterized and their C–C and C–heteroatom bond formation reactivity investigated. The $(^{R}N4)Ni^{II}$(cycloneophyl) derivatives have accessible oxidation potentials and thus can easily be oxidized with a variety of oxidants. Interestingly, oxidation of $(^{R}N4)Ni^{II}$(cycloneophyl) complexes with O_2 and H_2O_2 generates both C–C and C–O bond formation products. For example, the $(^{TsMe}N4)Ni^{II}$(cycloneophyl) complex yields C–O bond formation products in 41% yield, along with the C–C coupled product for an overall conversion of 94%. Cryo-ESI-MS studies were employed to detect high-valent Ni–oxygen species and a mechanism was proposed for the oxidatively-induced C–C and C–O bond formation reactions. Overall, the $(^{TsMe}N4)Ni^{II}$(cycloneophyl) complex seems to be at the sweet spot of stability *vs.* reactivity for C–O bond formation, while the $(^{Ts}N4)Ni^{II}$(cycloneophyl) complex gives the highest yield of C–C coupled product. All these results are very promising, suggesting that organometallic Ni complexes supported by multidentate ligands can exhibit bioinspired aerobic oxidation chemistry, which could be further developed into catalytic aerobic oxidative transformations.

Conflicts of interest

The authors declare no competing financial interest.

Acknowledgements

We thank the National Science Foundation (NSF CHE-1255424 and CHE-1925751) for support. The purchase of the Bruker EMX-PLUS EPR spectrometer was supported by the National Science Foundation (MRI, CHE-1429711) and we thank Dr Michael B. Watson for the EPR measurements. X. R. thanks the Generalitat de Catalunya for an ICREA-Acadèmia Award, and Serveis Tècnics de Recerca, Universitat de Girona is acknowledged for experimental support.

References

1 F. Diederich and P. J. Stang, *Metal-Catalyzed Cross-Coupling Reactions*, Wiley-VCH, Weinheim; New York, 1998.
2 A. d. Meijere and F. Diederich, *Metal-Catalyzed Cross-Coupling Reactions*, Wiley-VCH, Weinheim, New York, 2004.
3 J. F. Hartwig, *Organotransition Metal Chemistry: From Bonding to Catalysis*, University Science Books, Sausalito, 2010.
4 T. T. Tsou and J. K. Kochi, *J. Am. Chem. Soc.*, 1979, **101**, 7547–7560.
5 M. R. Netherton and G. C. Fu, *Adv. Synth. Catal.*, 2004, **346**, 1525–1532.
6 Y. Tamaru, *Modern Organonickel Chemistry*, Wiley-VCH, Weinheim, New York, 2005.
7 A. C. Frisch and M. Beller, *Angew. Chem., Int. Ed.*, 2005, **44**, 674–688.
8 V. B. Phapale and D. J. Cardenas, *Chem. Soc. Rev.*, 2009, **38**, 1598–1607.
9 A. Rudolph and M. Lautens, *Angew. Chem., Int. Ed.*, 2009, **48**, 2656–2670.
10 G. D. Jones, J. L. Martin, C. McFarland, O. R. Allen, R. E. Hall, A. D. Haley, R. J. Brandon, T. Konovalova, P. J. Desrochers, P. Pulay and D. A. Vicic, *J. Am. Chem. Soc.*, 2006, **128**, 13175–13183.
11 X. Hu, *Chem. Sci.*, 2011, **2**, 1867–1886.
12 Y. Aihara and N. Chatani, *J. Am. Chem. Soc.*, 2013, **135**, 5308–5311.
13 Y. Aihara and N. Chatani, *J. Am. Chem. Soc.*, 2014, **136**, 898–901.
14 Y. Aihara, M. Tobisu, Y. Fukumoto and N. Chatani, *J. Am. Chem. Soc.*, 2014, **136**, 15509–15512.
15 B. Zheng, F. Tang, J. Luo, J. W. Schultz, N. P. Rath and L. M. Mirica, *J. Am. Chem. Soc.*, 2014, **136**, 6499–6504.
16 J. Cornella, J. T. Edwards, T. Qin, S. Kawamura, J. Wang, C. M. Pan, R. Gianatassio, M. Schmidt, M. D. Eastgate and P. S. Baran, *J. Am. Chem. Soc.*, 2016, **138**, 2174–2177.
17 H. W. Xu, J. B. Diccianni, J. Katigbak, C. H. Hu, Y. K. Zhang and T. N. Diao, *J. Am. Chem. Soc.*, 2016, **138**, 4779–4786.
18 N. M. Camasso, A. J. Canty, A. Ariafard and M. S. Sanford, *Organometallics*, 2017, **36**, 4382–4393.
19 F. D'Accriscio, P. Borja, N. Saffon-Merceron, M. Fustier-Boutignon, N. Mezailles and N. Nebra, *Angew. Chem., Int. Ed.*, 2017, **56**, 12898–12902.
20 J. P. Cloutier and D. Zargarian, *Organometallics*, 2018, **37**, 1446–1455.
21 K. Koo and G. L. Hillhouse, *Organometallics*, 1995, **14**, 4421–4423.
22 K. M. Koo, G. L. Hillhouse and A. L. Rheingold, *Organometallics*, 1995, **14**, 456–460.
23 R. Y. Han and G. L. Hillhouse, *J. Am. Chem. Soc.*, 1997, **119**, 8135–8136.
24 E. Kogut, H. L. Wiencko, L. B. Zhang, D. E. Cordeau and T. H. Warren, *J. Am. Chem. Soc.*, 2005, **127**, 11248–11249.
25 V. Pandarus and D. Zargarian, *Organometallics*, 2007, **26**, 4321–4334.
26 V. Pandarus and D. Zargarian, *Chem. Commun.*, 2007, 978–980, DOI: 10.1039/b613812h.
27 D. M. Spasyuk, D. Zargarian and A. van der Est, *Organometallics*, 2009, **28**, 6531–6540.
28 A. T. Higgs, P. J. Zinn and M. S. Sanford, *Organometallics*, 2010, **29**, 5446–5449.
29 N. M. Camasso and M. S. Sanford, *Science*, 2015, **347**, 1218–1220.
30 T. Corona, A. Draksharapu, S. K. Padamati, I. Gamba, V. Martin-Diaconesou, F. Acuna-Pares, W. R. Browne and A. Company, *J. Am. Chem. Soc.*, 2016, **138**, 12987–12996.
31 J. R. Bour, N. M. Camasso, E. A. Meucci, J. W. Kampf, A. J. Canty and M. S. Sanford, *J. Am. Chem. Soc.*, 2016, **138**, 16105–16111.
32 G. E. Martinez, C. Ocampo, Y. J. Park and A. R. Fout, *J. Am. Chem. Soc.*, 2016, **138**, 4290–4293.
33 H. Lee, J. Borgel and T. Ritter, *Angew. Chem., Int. Ed.*, 2017, **56**, 6966–6969.
34 J. B. Diccianni, C. H. Hu and T. N. Diao, *Angew. Chem., Int. Ed.*, 2017, **56**, 3635–3639.
35 M. B. Watson, N. P. Rath and L. M. Mirica, *J. Am. Chem. Soc.*, 2017, **139**, 35–38.
36 E. A. Meucci, N. M. Camasso and M. S. Sanford, *Organometallics*, 2017, **36**, 247–250.
37 J. R. Khusnutdinova, N. P. Rath and L. M. Mirica, *J. Am. Chem. Soc.*, 2010, **132**, 7303–7305.
38 J. R. Khusnutdinova, N. P. Rath and L. M. Mirica, *Angew. Chem., Int. Ed.*, 2011, **50**, 5532–5536.
39 J. R. Khusnutdinova, N. P. Rath and L. M. Mirica, *J. Am. Chem. Soc.*, 2012, **134**, 2414–2422.
40 F. Z. Tang, Y. Zhang, N. P. Rath and L. M. Mirica, *Organometallics*, 2012, **31**, 6690–6696.
41 F. Tang, F. Qu, J. R. Khusnutdinova, N. P. Rath and L. M. Mirica, *Dalton Trans.*, 2012, **41**, 14046–14050.
42 F. Qu, J. R. Khusnutdinova, N. P. Rath and L. M. Mirica, *Chem. Commun.*, 2014, **50**, 3036–3039.
43 B. Zheng, F. Tang, J. Luo, J. W. Schultz, N. P. Rath and L. M. Mirica, *J. Am. Chem. Soc.*, 2014, **136**, 6499–6504.
44 J. R. Khusnutdinova, N. P. Rath and L. M. Mirica, *Inorg. Chem.*, 2014, **53**, 13112–13129.
45 A. J. Wessel, J. W. Schultz, F. Tang, H. Duan and L. M. Mirica, *Org. Biomol. Chem.*, 2017, **15**, 9923–9931.
46 C. M. Che, Z. Y. Li, K. Y. Wong, C. K. Poon, T. C. W. Mak and S. M. Peng, *Polyhedron*, 1994, **13**, 771–776.
47 J. Campora, J. A. Lopez, P. Palma, D. del Rio, E. Carmona, P. Valerga, C. Graiff and A. Tiripicchio, *Inorg. Chem.*, 2001, **40**, 4116–4126.
48 J. Campora, M. D. Conejo, K. Mereiter, P. Palma, C. Perez, M. L. Reyes and C. Ruiz, *J. Organomet. Chem.*, 2003, **683**, 220–239.
49 J. W. Schultz, K. Fuchigami, B. Zheng, N. P. Rath and L. M. Mirica, *J. Am. Chem. Soc.*, 2016, **138**, 12928–12934.
50 See the ESI†
51 J. R. Bour, N. M. Camasso and M. S. Sanford, *J. Am. Chem. Soc.*, 2015, **137**, 8034–8037.
52 E. Chong, J. W. Kampf, A. Ariafard, A. J. Canty and M. S. Sanford, *J. Am. Chem. Soc.*, 2017, **139**, 6058–6061.

53 M. D. Aseman, S. M. Nabavizadeh, F. N. Hosseini, G. Wu and M. M. Abu-Omar, *Organometallics*, 2018, **37**, 87–98.
54 F. C. S. E. Silva, A. F. Tierno and S. E. Wengryniuk, *Molecules*, 2017, **22**, 780.
55 A. Company, S. L. Yao, K. Ray and M. Driess, *Chem.–Eur. J.*, 2010, **16**, 9669–9675.
56 S. K. Padamati, D. Anielone, A. Draksharapu, G. Primi, D. J. Martin, M. Tromp, M. Swart and W. R. Browne, *J. Am. Chem. Soc.*, 2017, **139**, 8718–8724.
57 E. M. Prokopchuk, H. A. Jenkins and R. J. Puddephatt, *Organometallics*, 1999, **18**, 2861–2866.
58 E. M. Prokopchuk and R. J. Puddephatt, *Can. J. Chem.*, 2003, **81**, 476–483.
59 V. V. Rostovtsev, L. M. Henling, J. A. Labinger and J. E. Bercaw, *Inorg. Chem.*, 2002, **41**, 3608–3619.
60 P. L. Alsters, H. T. Teunissen, J. Boersma, A. L. Spek and G. van Koten, *Organometallics*, 1993, **12**, 4691–4696.
61 A. J. Canty, H. Jin, A. S. Roberts, B. W. Skelton and A. H. White, *Organometallics*, 1996, **15**, 5713–5722.
62 A. N. Vedernikov, *Acc. Chem. Res.*, 2012, **45**, 803–813.